

Supporting Information

Achieving highly thermostable red emission in singly Mn²⁺-doped BaXP₂O₇ (X = Mg/Zn) via self-reduction

Song Li^a, Wei Hu^a, Mikhail G. Brik^{b,c,d,e,*}, Shixun Lian^a, Zhongxian Qiu^{a,*}

^aKey Laboratory of Light Energy Conversion Materials of Hunan Province College, Key Laboratory of Chemical Biology & Traditional Chinese Medicine Research (Ministry of Education), College of Chemistry and Chemical Engineering, Hunan Normal University, Changsha 410081, China

*Corresponding author: zxqiu@hunnu.edu.cn (Z. Qiu)

^bInstitute of Physics, University of Tartu, W. Ostwald Str. 1 Tartu 50411, Estonia

*Corresponding author: mikhail.brik@ut.ee (M. G. Brik)

^cSchool of Optoelectronic Engineering & CQUPT-BUL Innovation Institute, Chongqing University of Posts and Telecommunications, Chongqing 400065, People's Republic of China

^dFaculty of Science and Technology, Jan Długosz University, Armii Krajowej 13/15, PL-42200 Częstochowa, Poland

^eAcademy of Romanian Scientists, Ilfov Str. No. 3, 050044, Bucharest, Romania

The BaZn_{1-x}P₂O₇:xMn²⁺ (BZPO:xMn; x = 0.10–0.24) phosphors show gradual reduced XRD peak intensities with increasing Mn content indicating lowering crystallinity of the powders. We propose the more Mn²⁺-doping leads to increased defect concentration in the host compound so that the crystal structure needs higher temperature to achieve newly thermodynamic stable state. As comparison, we prepared the BZPO:xMn²⁺ (x = 0.16, 0.18, 0.20, 0.22, 0.24) samples at 950 and 1000 °C, respectively. The XRD patterns of the samples at 950 °C are displayed in **Fig. S1a**, which show higher peak intensities than those at 900 °C, confirming the hypothesis of the newly thermodynamic stable structure with large defect concentration. Meanwhile, a further increase of the synthetic temperature to 1000 °C is too high to convert the

powder samples to glassy state.

In addition, the large Mn^{2+} incorporation and elevated temperature will facilitate the structural transformation from BaZnP_2O_7 to BaMnP_2O_7 so that the $\text{BZPO}:x\text{Mn}^{2+}$ samples show some feature of BaZnP_2O_7 crystal in the case of high Mn^{2+} concentration, especially at elevated reaction temperature. As seen in **Fig. S1b**, in spite of the enhanced integral peak intensity at 950 °C than at 900 °C, the diffraction peaks ascribing to (020) and (1-21) planes rise faster than others in $\text{BZPO}:0.20\text{Mn}^{2+}$. Thus, we set the synthetic temperature at 900 °C for the $\text{BZPO}:x\text{Mn}^{2+}$ materials.

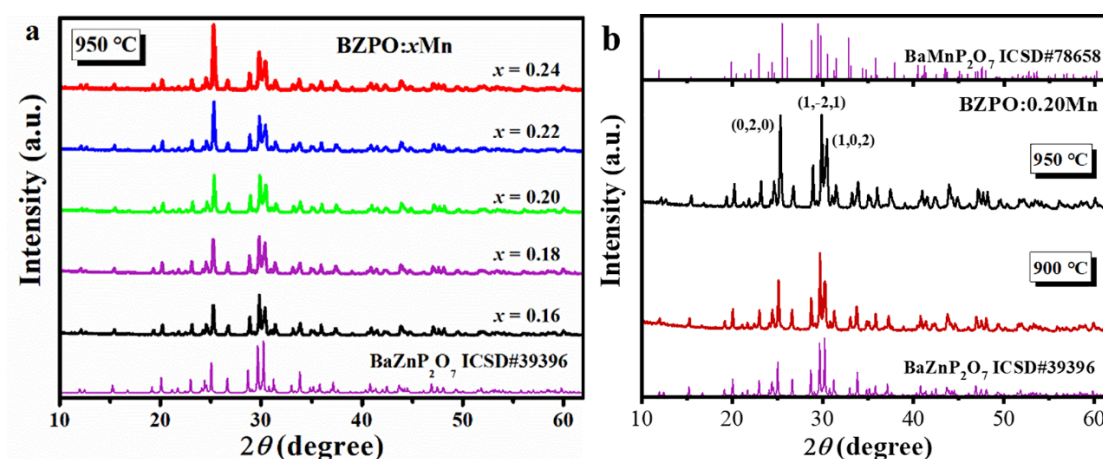


Fig. S1 (a) XRD patterns of $\text{BZPO}:x\text{Mn}$ ($x = 0.16\text{--}0.24$) synthesized at 950 °C; (c) The comparison of the XRD patterns of $\text{BZPO}:0.20\text{Mn}$ synthesized at different temperatures.

The ICP test verifies the stoichiometric compositions of the cations in $\text{BXPO}:0.20\text{Mn}^{2+}$ ($X = \text{Mg}/\text{Zn}$) phosphors as in the nominal formulas. The oxygen contents are estimated by subtracting the mass sum of the cationic components from the total mass of the test powder. This method to estimate the oxygen content may not be precise. As a result, the oxygen contents are both over stoichiometric ones in the two representative samples.

Table S1 Element contents of BXPO:0.20Mn²⁺ (X = Mg/Zn) phosphors by ICP

BMPO:0.20Mn ²⁺			BZPO:0.20Mn ²⁺		
Element	Mass (%)	Atom [mol%]	Element	Mass (%)	Atom [mol%]
Ba	37.28	0.93	Ba	36.37	0.99
Mg	5.61	0.79	Zn	13.78	0.79
Mn	2.82	0.18	Mn	2.64	0.18
P	16.07	1.78	P	14.75	1.78
O	38.22*	8.16*	O	32.46*	7.60*

* The oxygen contents were speculated according to the mass difference between the total mass of the test powder and the mass sum of the cations.

The CIE chromaticity coordinates confirm the red-emitting feature of the two types of red phosphors, which are (0.622, 0.387) for BMPO:0.20Mn²⁺ and (0.650, 0.350) for BZPO:0.20Mn²⁺ falling in the red region as shown in **Fig. S2**.

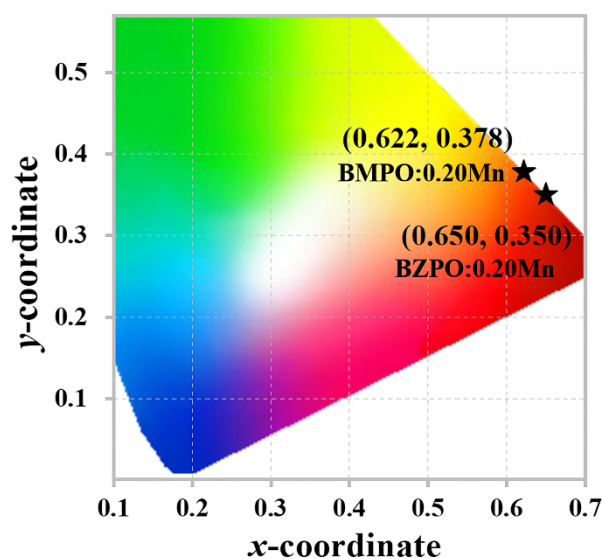


Fig. S2 CIE chromaticity coordinate diagram of BXPO:0.20Mn²⁺ (X = Mg/Zn);

Fig. S3 displays the full XPS spectra of BXPO:0.20Mn²⁺ (X = Mg/Zn), which prove the successful incorporation of Mn into BXPO host.

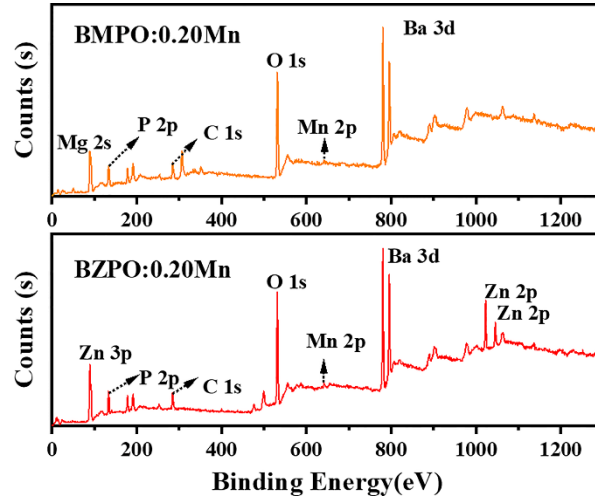


Fig. S3 The full XPS spectra of BXPO:0.20Mn²⁺ (X = Mg/Zn)

The nearest cations around X²⁺ (X = Mg/Zn) sites in BXPO are listed in **Table S2**. The smaller distance between nearest Mg²⁺—Ba²⁺ than Mg²⁺—Mg²⁺ indicates the cationic vacancy defects may occur mainly at Ba²⁺ sites for BMPO:Mn²⁺ during the self-reduction process for charge compensation due to the reasonable defect-pair interaction between $Mn_{Mg}^{\bullet\bullet} + V_{Ba}^{\bullet\bullet}$. The higher thermoluminescence intensity in Ba_{0.96}Mg_{0.8}P₂O₇:0.20Mn²⁺ (MnCO₃) than BaMg_{0.76}P₂O₇:0.20Mn²⁺ (MnCO₃) emphasizes the larger possibility of V_{Ba} than V_{Mg}. By contrast, there are two nearest Zn²⁺ sites around Zn²⁺ within 5 Å distance (the least distance beyond effective interaction of atoms) except for the four Ba²⁺ sites. Given the easy volatility of zinc, we presume the V_{Zn}^{••} defect also plays a great role as charge defect in BZPO:Mn²⁺, which is consistent with the stronger thermoluminescence and the corresponding denser charge defects in BZPO:Mn²⁺ than those in BMPO:Mn²⁺.

Table S2 The nearest cationic distribution around X^{2+} in $BaMgP_2O_7$ ($X = Mg/Zn$)

BaMgP₂O₇		BaZnP₂O₇	
X-cation	Distance (Å)	X-cation	Distance (Å)
Mg-Ba	3.7256	Zn-Ba	3.8048
	3.7484		3.9563
	4.0372		3.9892
	4.1650		4.7594
	4.1986		
Mg-Mg	4.8237	Zn-Zn	3.3060
	5.2445		4.0926
	5.4183		5.3270

Fig. S4a displays the decay curves of the $BZPO:Mn^{2+}$ ($MnCO_3$) phosphor. The luminescence decay curves prove exponential decay behaviors in $BZPO:Mn^{2+}$ ($MnCO_3$) through the temperature range of 300–550 K. Compared with $BMPO:Mn^{2+}$, the $BZPO:Mn^{2+}$ ($MnCO_3$) shows longer lifetime than, which is due to the thermal population of E state that is electric dipole symmetry-allowed in $BZPO:Mn^{2+}$ on consideration of the C_{4v} symmetric ligand field but not the case for any of the states in $BMPO:Mn^{2+}$. In addition, without the relative charge defect, the $BZPO:Mn^{2+}$ ($MnCO_3$) shows shorter lifetime than $BZPO:Mn^{2+}$ (MnO_2) (**Fig. S4b**).

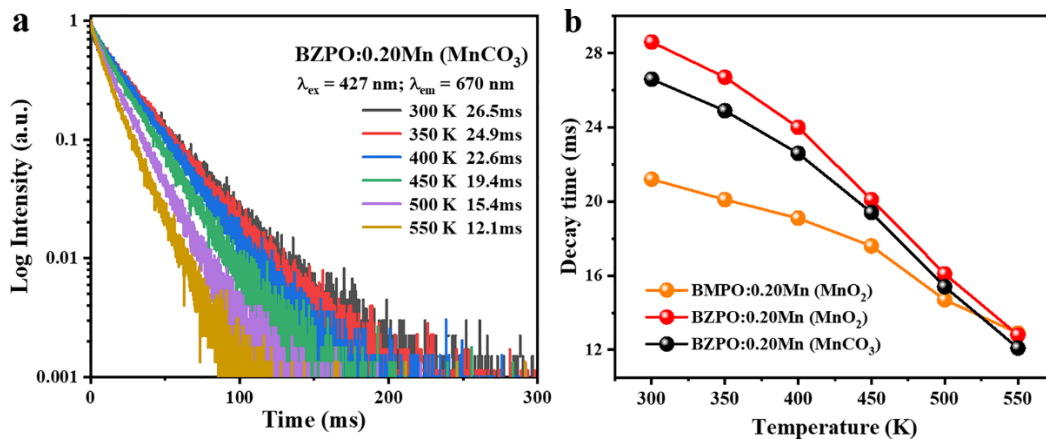


Fig. S4. (a) Temperature-dependent decay curves of $BZPO:0.20Mn^{2+}$ ($MnCO_3$); (b) The comparison of the decay times of $BMPO:0.20Mn^{2+}$ (MnO_2), $BZPO:0.20Mn^{2+}$ (MnO_2), and $BZPO:0.20Mn^{2+}$ ($MnCO_3$).